



Carbon uptake and water use in woodlands and forests in southern Australia during an extreme heat wave event in the ‘Angry Summer’ of 2012/2013.

Eva van Gorsel¹, Sebastian Wolf², Peter Isaac¹, James Cleverly³, Vanessa Haverd¹, Cécilia Ewenz⁴,
5 Stefan Arndt⁵, Jason Beringer⁶, Víctor Resco de Dios⁷, Bradley J. Evans⁸, Anne Griebel^{5,9}, Lindsay B.
Hutley¹⁰, Trevor Keenan¹¹, Natascha Kljun¹², Craig Macfarlane¹³, Wayne S. Meyer¹⁴, Ian McHugh¹⁵,
Elise Pendall⁹, Suzanne Prober¹³, Richard Silberstein¹⁶

1 CSIRO, Oceans and Atmosphere, Yarralumla, 2600, Australia

2 Department of Environmental Systems Science, ETH Zurich, 8092 Zurich, Switzerland

10 3 School of Life Sciences, University of Technology Sydney, Broadway, NSW, 2007, Australia

4 Airborne Research Australia, Flinders University, Salisbury South, SA, 5106, Australia

5 School of Ecosystem and Forest Sciences, The University of Melbourne, Richmond, 3121, Victoria, Australia

6 School of Earth and Environment (SEE), The University of Western Australia, Crawley, WA, 6009, Australia

7 Producció Vegetal i Ciència Forestal – Agrotecnio Centre, Universitat de Lleida, 25198, Lleida, Spain

15 8 School of Life and Environmental Sciences, The University of Sydney, Sydney, 2015, Australia

9 Hawkesbury Institute for the Environment, Western Sydney University, Penrith, NSW 2570

10 School of Environment, Research Institute for the Environment and Livelihoods, Charles Darwin University, NT, Australia

11 Lawrence Berkeley National Lab., 1 Cyclotron Road, Berkeley CA, USA

20 12 Dept of Geography, College of Science, Swansea University, Singleton Park, Swansea, UK

13 CSIRO Land and Water, Private Bag 5, Floreat 6913, Western Australia

14 Environment Institute, The University of Adelaide, Adelaide SA 5 005, Australia

15 School of Earth, Atmosphere and Environment, Monash University, Clayton, 3800, Australia

25 16 Centre for Ecosystem Management, Edith Cowan University, School of Natural Sciences, Joondalup, WA, 6027, Australia

Correspondence to: E. van Gorsel (eva.vangorsel@csiro.au)

Abstract. As a result of climate change warmer temperatures are projected through the 21st century and are already increasing above modelled predictions. Apart from increases in the mean, warm/hot temperature extremes are expected to become more prevalent in the future, along with an increase in the frequency of droughts. It is crucial to better understand
30 the response of terrestrial ecosystems to such temperature extremes for predicting land-surface feedbacks in a changing climate. During the 2012/2013 summer, Australia experienced a record-breaking heat wave with an exceptional spatial extent that lasted for several weeks. We synthesized eddy-covariance measurements from seven woodland and forest sites across climate zones in southern Australia, which we combined with model simulations from the CABLE land surface model to investigate the effect of this summer heat wave on the carbon and water exchange of terrestrial ecosystems. We found that



the water-limited woodlands and the energy-limited forest ecosystem responded differently to the heat wave. During the most intense part of the heat wave, the woodlands experienced decreased latent heat flux, an increased Bowen ratio and a reduced carbon uptake while the forest ecosystem had increased latent heat flux, reduced Bowen ratio and increased carbon uptake. Ecosystem respiration was increased at all sites resulting in reduced net ecosystem productivity in the woodlands and constant net ecosystem productivity in the forest. Importantly all ecosystems remained carbon sinks during the event. Precipitation after the most intense first part of the heat wave and slightly cooler temperatures led to a decrease of the Bowen ratio and hence increased evaporative cooling. Carbon uptake in the woodlands also recovered quickly but respiration remained high. While woodlands and forest proved relatively resistant to this short-term heat extreme these carbon sinks may not sustainable in a future with an increased number, intensity and duration of heat waves.

10 1 Introduction

Average temperatures in Australia have increased by 0.9°C since 1910 (CSIRO and BOM, 2014), which represents the most extreme of modeling scenarios, and further warming is projected with climate change (IPCC, 2013). In addition to increased mean temperature, warm temperature extremes are becoming more frequent in Australia and worldwide (Lewis and King, 2015, Steffen, 2015) and an increased prevalence of drought is expected for the future (Dai, 2013). Increases in temperature variability also affect the intensity of heat waves (Schär et al., 2004). Extreme heat and drought are often co-occurring (King et al. 2014), and soil water limitations can exacerbate the intensity of heat waves (Fischer et al., 2007; Seneviratne et al., 2010) due to reduced evaporative cooling and increased sensible heat flux (Sheffield et al., 2012). This combination of reduced water availability and increased evaporative demand places increased stress on terrestrial ecosystems.

During summer 2012/2013, Australia experienced a record-breaking heat wave that was deemed unlikely without climate change (Steffen, 2015). The Australian summer 2012/2013 was nicknamed the ‘Angry Summer’ or the ‘Extreme Summer’, as an exceptionally extensive and long-lived period of high temperatures affected large parts of the continent in late December 2012 and the first weeks of January 2013 (Bureau of Meteorology, BOM, 2013). Records were set in every Australian State and Territory and the record for the hottest daily average temperature (32.4°C) for Australia was recorded on the 8th of January (Karoly et al., 2013). On the Western Australian South Coast, the maximum temperature record was broken in Eucla on the 3rd of January with 48.2°C. In South Australia maximum temperature records were broken at four weather stations between the 4th and 6th of January. Victoria also observed record heat on the 4th of January at its south coast in Portland (42.1°C). In New South Wales, record temperatures were recorded on the 5th of January and were broken again on the 19th, reaching 46.2°C before the heat wave subsided. Besides being the hottest year since 1910, the summer 2012/2013 was also considerably drier than average in most parts of the continent, but particularly in the densely populated east. King et al. (2014) have shown that extreme heat was made much more likely by contributions from the very dry conditions over the inland eastern region of Australia as well as by anthropogenic warming.



Heat waves are becoming hotter, they last longer, and they occur more often (Steffen, 2015). As many ecological processes are more sensitive to climate extremes than to changes in the mean state (Hanson et al. 2006), it is imperative to understand the effect of climate extremes in order to predict the impact on terrestrial ecosystems. Processes and sensitivities differ among biomes, but forests are expected to experience the largest detrimental effects and the longest recovery times from climate extremes due to their large carbon pools and fluxes (Frank et al. 2015). While climate change generally increases the sink strength of terrestrial ecosystems through carbon dioxide and nitrogen fertilisation, there is increasing evidence that climate extremes can lead to a decrease in carbon uptake and carbon stocks thus having the potential to counteract an expected increase in terrestrial carbon uptake with climate change (Zhao and Running, 2010, Reichstein et al., 2013). It is therefore crucial to better understand the ecosystem response to climate extremes. The role of climate extremes could be critical in shaping future ecosystem dynamics (Zimmermann et al. 2009), but the sporadic and unpredictable nature of these events makes it difficult to monitor how they affect vegetation through space and time (Mitchell et al., 2014).

Australian forest and woodland ecosystems are strongly influenced by large climatic variability with recurring drought events and heat waves (Beringer et al., 2016, Mitchell et al., 2014). *Eucalyptus regnans* ecosystems in southeast Australia, for example, have an exceptional capacity to withstand drought and recover quickly after heat waves (Pfausch and Adams, 2013). However, drought and heat related forest die-back events have also been observed in southwestern Australia (Matusick et al. 2013, Evans and Lyons 2013), where drought stress from long-term reductions in rainfall was exacerbated by short heat wave periods. This suggests that these ecosystems, even though they are resilient to dry and hot conditions, are susceptible to mortality events once key thresholds have been exceeded (Evans et al., 2013). Large-scale droughts and heat waves in Europe during 2003 (Ciais et al., 2005) and in the US during 2012 (Wolf et al. 2016) caused substantial reductions in summer carbon uptake, and vegetation-climate feedbacks were found to contribute to enhanced temperatures (Teuling et al. 2010). However, direct observations of the ecosystem response to large-scale extremes in Australia are lacking.

The large extent of the high temperatures in early 2013 across Australia and direct observations from the OzFlux network now enable us to analyse the effect of extreme hot and dry conditions on the carbon, water and energy cycles of the major woodland and forest ecosystems in the southern parts of Australia. In this study, we combined eddy-covariance measurements from seven woodland and forest sites with model simulations from BIOS2 (Haverd et al. 2013) to investigate the impact of the 2012/2013 summer heat wave and drought on the carbon and water exchange of terrestrial ecosystems across climate zones in southern Australia and assess the influence of land-surface feedbacks on the magnitude of the heat wave.



2 Materials and Methods

We compared hourly data from seven OzFlux sites (Fig. 1, Table 1) measured during the heat wave period 1/1/2013 – 18/1/2013 with observations from a background reference. We used eddy covariance data to compare hourly data and the daily cycle of the relevant fluxes. We used a reference period (BGH) one year later from 2/1/2014 – 6/1/2014. During these 5 time periods all towers were actively taking measurements, while in 2013 for both earlier and later time periods, data were not available for all sites at the time of data analysis. The reference period is shorter than the heat wave period because another significant heat wave event affected southeastern Australia later in January 2014 and at the end of 2013 not all sites had data available. Temperatures during the background reference period were also somewhat warmer than average climatology (Fig. 3). We therefore expect the relative severity of the effects of the heat wave to appear smaller than they 10 otherwise would when compared against a climatological reference. To ensure the representativeness of our results, we also compared daily data against a climatology derived from daily BIOS2 (see below) output for the time period 1982-2013 (background climatology, BGC). BIOS2 results for the whole time period are only available as daily values.

2.1 Sites

We analysed data from seven southern Australian sites (Beringer et al., 2016) grouped in three distinct ecosystem and 15 climate types: Mediterranean woodlands (MW), temperate woodlands (TW) and temperate forests (TF) (Fig. 1, Table 1).

MW sites included i) a coastal heath *Banksia* woodland (AU-Gin) ii) a semi-arid eucalypt woodland dominated by *Eucalyptus salmonophloia* (Salmon gum), with *E. salubrious* (Gimlet) and other eucalypts (AU-Gww); and iii) AU-Cpr, which is situated in a semi-arid mallee ecosystem, which is characterised by an association of mallee eucalypts (*E. dumosa*, 20 *E. incrassata*, *E. oleosa* and *E. socialis*) with spinifex hummocks (*Triodia basedowii*) (Sun et al. 2015, Meyer et al., 2015). TW sites are classified as dry sclerophyll and include i) AU-Wom, which is a secondary re-growth of *E. oblique* (Messmate Stringybark), *E. radiata* (Narrow-Leaved Peppermint) and *E. rubida* (Candlebark). ii) AU-Whr is a box woodland mainly composed of *E. microcarpa* (Grey Box) and *E. leucoxylon* (Yellow Gum). Smaller numbers of *E. sideroxylon* (Ironbark) and *Acacia pycnantha* (Golden Wattle) also occur on site. iii) In Cumberland Plains (AU-Cum) the canopy is dominated by *E.* 25 *moluccana* and *E. fibrosa*, which host an expanding population of *Amyema miquelii* (mistletoe). Temperate Forests (TF) are represented by the Tumbarumba site (AU-Tum), which is in a wet sclerophyll forest dominated by *E. delegatensis* and *E. dalrympleana* (Leuning et al., 2005).

The sites fall into the classifications “Mediterranean Forests, Woodland and Scrub” (AU-Gin, AU-GWW and AU-Cpr) or 30 the “Temperate Broadleaf and Mixed Forest” (AU-Wom, Au-Cum, AU-Whr and AU-Tum) classifications of IBRA (Interim Biogeographic Regionalisation for Australia v. 7, (Environment, 2012)). In temperate Australia both woodlands and forests are mainly dominated by Eucalyptus species. Forests occur in the higher rainfall regions and woodlands form the transitional



zone between grass-shrublands and forests and the dried interior. We therefore classified temperature ecosystems with mean annual precipitation > 1000mm and tree height > 30m as woodlands. None of the sites is continental but elevation ranges from 33m asl (AU-Cum) to 1260 m asl (AU-Tum). The mean annual temperature for the years 1982 - 2013 ranged from 9.8 °C in AU-Tum to 18.7°C in AU-Gww (Table 1). Mean annual precipitation also covers a large range from 265 mm year⁻¹ in 5 AU-Cal to 1417 mm year⁻¹ in AU-Tum.

2.2 OzFlux Data

We analysed data collected by the OzFlux network (www.OzFlux.org.au). Each site has a set of eddy covariance (EC) instrumentation, consisting of an infrared gas analyser (LI-7500 or LI-7500A, LI-COR, Lincoln, NE, USA) and a 3D sonic anemometer (generally a CSAT3 (Campbell Scientific Instruments, Logan, UT, USA) except for AU-Tum, where a Gill-HS is operational (Gill Instruments, Lymington, UK)). Supplementary meteorological observations include radiation (4 component CNR4 or CNR1, Kipp and Zonen, Delft, Netherlands) and temperature and humidity (HMP 45C or HMP50, Vaisala, Helsinki, Finland). Soil volumetric water content was measured with CS616 (Campbell Scientific). EC data were processed using the OzFlux-QC processing tool (Isaac et al., 2016). Processing steps and corrections included outlier 15 removal, coordinate rotation (double rotation), frequency attenuation correction, conversion of virtual heat flux to sensible heat flux, and the WPL correction (Tanner and Thurtell, 1969, Wesley, 1970, Webb et al., 1980, Schotanus et al., 1983, Lee et al. 2004 and references therein). Friction velocity thresholds were calculated following the method of Barr et al. (2013). In Tumberumba, where advection issues are known (van Gorsel et al., 2007, Leuning et al. 2008), only data from the early evening was used during nighttime hours (van Gorsel, 2009). Gaps in the meteorological time series were filled using 20 alternate data sets, BIOS2 or ACCESS (Australian Community Climate and Earth-System Simulator) output or climatologies (usually in this order of preference). Gaps in the flux time series were filled using a self-organising linear output model (SOLO-SOFM, Hsu et al., 2002, Abramowitz et al. 2006 and references therein). The OzFlux data used in this analysis are available from <http://data.ozflux.org.au/portal/>.

25 2.3 BIOS2

The coupled carbon and water cycles were modeled using BIOS2 (Haverd et al., 2013a; Haverd et al., 2013b) constrained by multiple observation types, and forced using remotely sensed vegetation cover. BIOS2 is a fine-spatial-resolution (0.05 degree) offline modelling environment, including a modification of the CABLE biogeochemical land surface model (Wang et al., 2011; Wang et al., 2010) incorporating the SLI soil model (Haverd and Cuntz, 2010). BIOS2 parameters are 30 constrained and predictions are evaluated using multiple observation sets from across the Australian continent, including streamflow from 416 gauged catchments, eddy flux data (CO₂ and H₂O) from 14 OzFlux sites (Isaac, 2015), litterfall data, and soil, litter and biomass carbon pools (Haverd et al., 2013a). In this work, we updated BIOS2 to use the GIMMS3g



FAPAR product (Zhu et al., 2013) for prescribed vegetation cover. The reference period used, BGC, is 1982-2013, the period over which remotely sensed data is available.

2.4 Analyses

5 All data analyses were performed using Python 2.7.11 and the Anaconda (4.0.0) distribution by Continuum Analytics using jupyter notebooks. Differences between heat waves and reference periods were determined by calculating z-scores of temperatures and soil water during the relevant periods. z-scores represent the number of standard deviations an observation is above or below the mean, depending upon the sign of the z-score. These were calculated with the z-score function of the scipy stats module for the period 1st-18th January relative to the mean across all years in the BIOS2 output (1982-2014). The
10 scipy stats functions bartlett and ttest_ind were used to determine the significance of differences of a range of variables between the background period (BGH or BGC) and the heat wave periods HW1 (1/1/2013-9/1/2013) and HW2 (HW2, 10/1/2013-18/1/2013). Boxplots were created using Matplotlib.

2.5 Conventions

We use the terminology and concepts as introduced by Chapin et al. (2006), where net and gross carbon uptake by vegetation
15 (net ecosystem production (NEP) and gross primary production (GPP)) are positive directed toward the surface and carbon loss from the surface to the atmosphere (ecosystem respiration (ER)) is positive directed away from the surface.

3 Results

3.1 Heat wave characterisation

The heat wave event commenced on the 25th of December 2012 with a build-up of extreme heat in the southwest of Western
20 Australia. A high pressure system in the Great Australian Bight and a trough near the west coast directed hot easterly winds over the area (BOM, 2013). From December 31 the high pressure system started moving eastwards and entered the Tasman Sea off eastern Australia on January 4th. The northerly winds directed very hot air into south eastern Australia. Temporary cooling was observed in the eastern states after the 8th of January, but in the meantime a second high pressure system moved into the Bight, starting a second wave of record breaking heat across the continent. The heat wave finally ended on the 19th
25 of January, when southerly winds brought cooler air masses to southern Australia.

Figure 2 shows the meteorological conditions at the sites during the heat wave. High temperatures at all sites were accompanied by high vapour pressure deficits. Soil water was very low in MW but increased at AU-Gin and particularly at AU-Gww after synoptic rainfalls around the 12th of January. The same, but less pronounced, was also the case for the TW
30 sites with similar soil water increases observed particularly at AU-Cum. At the TF site, Au-Tum, soil water decreased



throughout the heat wave (HW). Due to intermittent precipitation events we analysed two parts of the heat wave separately: heat wave period 1 (HW1, 1st–9th of January 2013) was characterised by very little precipitation and had low soil water at many sites. During heat wave period 2 (HW2, 10th–18th of January 2013) precipitation occurred at most sites (12th–15th January 2013) and resulted in increased soil water and lower temperatures than during HW1.

5

Temperatures were unusually high for the time of year at all sites (Fig 3). During HW1 they were generally more than 1.5-2 standard deviations (σ) higher than during the same time during the 32 years mean from the background period (BGC). At AU-Tum and AU-Gww z-scores even exceeded $+2\sigma$. During HW2 all sites showed lower z-scores for temperatures but they were still more than $+1\sigma$ higher than average temperatures. The background period BGH, against which we compare the hourly data of the heat wave, was also warmer than average conditions during the past 30 years but for most sites these z-scores were well below 1.

Soil water content was unusually low for the time of year. It was mostly more than -1σ below average, except at AU-Gww where soil water content was higher than average during HW2. All sites except the AU-Gin and AU-Gww had a lower z-score for soil water during HW2 than HW1, indicating relatively drier conditions with respect to the climatology despite the presence of rainfall during HW2. The background period BGH was generally less dry than the heat wave periods, one noteworthy exception being AU-Tum, which had very dry conditions (-2σ) during BGC in early January 2014. The z-scores indicate that high temperatures were more unusual than low soil water during HW1. HW2 was both hot and dry.

3.2 Ecosystem response to dry and hot conditions

3.2.1 Energy Exchange

Incoming and reflected short-wave radiation were only significantly increased in the energy limited ecosystem AU-Tum during the first period of the heat wave (Fig. 4, Table 2). Otherwise they remained approximately the same as BGH values except at the MW sites, where they were even significantly reduced during HW2 (Table 2). The relatively short duration of the extreme heat wave did not result in changes in albedo (not shown). A warmer atmosphere and potentially increased cloud cover led to an increase in longwave downward radiation in Western Australia. Due to increased surface temperatures longwave radiation emitted at the land surface was significantly increased at all sites for both heat wave periods, though more so during HW1. Significantly reduced net radiation was only measured at MW sites during HW2. At all other sites, net radiation was approximately the same during HW1, HW2 and BGH. Available energy (not shown) was significantly reduced at MW and TW sites during HW1 but was about the same for HW2 and the TF site.

30

Figure 5 demonstrates how remarkably different the energy partitioning was at MW, TW and TF sites, as we would expect given the wide climatological and biogeographic differences (Beringer et al., 2016). While similar fractions of energy went



into latent and sensible heat at the TF site, more energy was directed into sensible heat at TW sites. This energy flux partitioning towards sensible heat was even more pronounced at MW sites, where both the mean and the variability of latent heat flux were very small due to severe water limitations. Most of the available energy was transferred as sensible heat and hence contributed to the warming of the atmosphere.

5

During HW1, the variability and the daily average of the generally small latent heat flux at the MW sites were reduced even further (see also Table 2). During HW2, precipitation and temporarily increased water availability brought the latent heat flux back to levels observed during BGH. The latent heat flux did not change significantly at TW sites during the HWs compared to BGH conditions. At TF, however, the latent heat flux strongly increased. This was partly due to the very dry conditions in the background period BGH, but daily latent heat flux (F_e) was also increased compared to the climatology (BGC, Fig. A2), particularly during HW1.

10

The observed ratio of sensible to latent heat, the Bowen ratio (β , Bowen, 1926), was very large in the Mediterranean woodlands (Fig. 6). Typical values for β reach 6 for semi-arid to desert areas (e.g. Oliver, 1987, Beringer and Tapper, 2000). While this value was exceeded at MW even during BGH conditions, it increased to values larger than 10 during the heat wave. With rainfall and an increased latent heat flux, β decreased to below background conditions in HW2. In TW, β was higher than background values but decreased to similar values during HW2. At TF, β was lower than during the background period. It increased steadily in the morning and declined towards the evening and was quite symmetric, while in TW β increased strongly in the afternoon during the heat waves. This increase of β towards the afternoon hours was observed in MW during all time periods (including BGH).

15

20

Measured daily latent heat fluxes and β were consistent with flux climatology derived from BIOS2 during the background (BGH) (Fig. A1).

3.2.2 Carbon Exchange

Patterns of carbon fluxes were similar to between-site patterns of energy fluxes (Fig. 7, note differences in y-axes). All sites showed that maximum carbon uptake (GPP) occurred in the morning, decreased throughout the afternoon, and mostly increased again in the late afternoon. NEP followed the diurnal course of GPP, with the offset related to total ecosystem respiration (ER). ER increased with temperature and reached a maximum in the early afternoon (not shown).

25

Carbon uptake was significantly reduced at MW and TW during HW1 (Fig. 8). In TF, however, carbon uptake was increased during HW1 and HW2. Ecosystem respiration increased significantly in both periods of the heat wave and across all

30



ecosystems. Consequently, net ecosystem productivity was significantly reduced at MW and TW sites during both heat wave periods and unchanged at the TF site during HW1, but increased during HW2.

5 Measured GPP and ER showed the same responses in carbon uptake and losses during the heat waves as the flux climatology (BGC) derived with BIOS2 (Fig. A2): GPP was reduced during HW1 in woodland ecosystems and increased in the forest during both heat wave periods. ER was increased at all sites and during HW1 and HW2 compared to the long-term climatology.

4 Discussion

10 Persistent anticyclonic conditions led to heat wave conditions by bringing warm air from the interior of the continent to southern Australia. Such synoptic conditions are the most common weather pattern for associated with Australian heat waves (Steffen et al., 2014). Anticyclonic conditions also caused the intense 2003 European heat wave (Black et al., 2004) as well as the even more intense and widespread heat wave that reached across Eastern Europe, including western Russia, Belarus, Estonia, Latvia, and Lithuania in 2010 (Dole et al. 2011). Less cloud coverage and more clear sky conditions strongly increased incoming radiation (e.g. Black et al. 2004) and available energy during the European heat wave and drought in 15 2003 (Teuling et al., 2010), as well as during the recent drought and heat in California (Wolf et al., in review). During the 2012-2013 Australian heat wave, however, net radiation and available energy were similar or even reduced compared to background conditions, presumably due to increased cloud cover. Instead of more available energy to feed into turbulent heat fluxes, the drier sites (MW, TW) particularly experienced a reduction in the turbulent energy fluxes compared to background conditions. At TF, soil water was not limiting and given that the amount of available energy did not differ 20 significantly between BGH and both HW periods, the observed increase in latent heat flux was likely driven by increases in vapour pressure deficit (VPD), which is strongly correlated with the larger diurnal temperature range.

The Bowen ratio (β) increased at drier sites (MW and TW) and decreased at the TF site during the first part of the heat wave (HW1). Following rainfall between the two heat wave periods, β at the MW sites decreased to below background values, 25 while it was similar to background values in the TW. This was different compared to the observations made during the European heat wave in 2003. Teuling et al. (2010) observed that the surplus energy led to increases in both latent and sensible heat fluxes: over grassland, the energy was preferentially used to increase the latent heat flux (F_e), thereby decreasing β , whereas forest ecosystems generally had a stronger increase in the sensible heat flux (F_h) and an increase in β . They attributed the increase of the sensible heat flux and the Bowen ratio in forests to reduced water loss by forest 30 ecosystems due to stomatal regulation. The diurnal cycle of β at the MW sites generally showed an increase of β towards the afternoon hours. This increase was more pronounced during the heat wave periods than during BGH indicating the presence of stomatal control. At TW sites, β only had pronounced asymmetry during heat waves, clearly showing stronger stomatal



control than during background conditions. At the TF site, β was lower during both heat waves and the symmetry in β indicates that the decrease in midday stomatal conductance was either counteracted by a steadily increasing humidity deficit with rising temperatures from morning to mid-afternoon (Tuzet et al. 2003), or that there was little stomatal control of the latent heat flux at this site, or a combination of both.

5

Increased latent heat flux in response to increased temperature, vapour pressure deficit (MW, TW and TF) and solar radiation (TF) suppresses further heating of the atmosphere (Teuling et al., 2010), as long as latent heat flux is not limited by soil water during the period of peak insolation in summer (Wolf et al. 2016). At TF the relative extractable water was above a threshold of 0.4 for all but the last two days of the heat wave (not shown) indicating that for most of the time soil water was not limiting the latent heat flux (Granier et al., 1999). Latent heat suppresses further heating of the atmosphere but without precipitation depletes soil moisture at the site. Depleted soil water stores lead to a positive feedback as more energy goes into the sensible than the latent heat flux further increasing temperatures and amplifying the heat extremes (Whan et al. 2015). This is important as the joint occurrence of high temperatures and drought typically play a crucial role in tree mortality and forest die-back (Mitchell et al., 2014; Evans et al, 2013).

15

Temperature extremes can affect both photosynthesis and respiration (Frank et al., 2015). We observed a diurnal asymmetry in GPP at all sites and in all measurement periods. This is expected in ecosystems that exert some degree of stomatal control to avoid excessive reductions in water potential (e.g. in the afternoon), during higher atmospheric demand and the reduced ability of the soil to supply this water to the roots because of lower matrix potentials and hydraulic conductivity (Tuzet et al. 2003). During HW1, the time of maximum carbon uptake was earlier in the morning at the woodland sites MW and TW, and we observed strongly reduced carbon uptake throughout the day. This is consistent with observations made during e.g. the 2003 European heat wave (Ciais et al. 2005), the 2010 European heat wave (Guerlet, 2013), and the 2013 heat wave and drought that affected large parts of Southern China (Yuan et al. 2015). During these heat waves, carbon uptake was strongly reduced in general. During HW2, however, the shift of maximum GPP toward earlier hours of the day was less pronounced at MW and TW, thus daytime carbon uptake was not significantly reduced. This was in response to the intermittent precipitation and somewhat lower temperatures, which led to a reduction in vapour pressure deficit and increased soil water availability (Fig. 2). At the TF site, however, carbon uptake was significantly increased during both periods of the heat wave (see also Fig. 7). This can partly be explained by the very dry conditions during the background period, which could have caused below average carbon uptake, although the comparison against the long-term climatology also showed increased carbon uptake during HW1 and HW2. With temperatures clearly above an optimum temperature for carbon uptake and VPD exceeding values where stomatal closure can be expected at this site (van Gorsel et al. 2013), increased incoming shortwave radiation and potentially increased photosynthetically active leaf area likely have led to an increased carbon uptake in this typically energy limited ecosystem.

25
30



Increases in ER during the heat wave seem intuitive, given the exponential response of respiration to temperature (e.g. Richardson et al., 2006). However, drought can override the positive effect of warmer temperatures and lead to reduced respiration due to water limitations, as observed during the 2003 heat wave in Europe (Reichstein et al., 2007). The increased air and soil temperatures during both heat waves led to significantly increased ecosystem respiration at all sites. This led to significantly lower NEP in MW ecosystems when combined with reductions in GPP during HW1 and GPP not being significantly different from background GPP during HW2. At the TF site AU-Tum the increase in GPP during HW2 outweighed the increase in ecosystem respiration and NEP increased during this time period compared to the background.

Importantly, all sites remained carbon sinks during both heat waves periods. However, future increases in the number, intensity and duration of heat waves could turn the Mediterranean and temperate woodlands into carbon sources, leading to a positive carbon-climate feedback. Heat waves can induce a transition from energy-limited to water-limited ecosystems (Zscheischler et al. 2015). Transitioning toward more water limitation, especially for energy-limited forests, can exacerbate the deleterious effects of extreme events. Recurrent non-catastrophic heat stress can lead to increased plant mortality, the impact of which would be more evident over longer timescales (McDowell et al., 2008), and an increase in the frequency of fires (Hughes, 2003). Future climate change is also likely to be accompanied by increased plant water use efficiency due to elevated CO₂ (Keenan et al., 2013), which could lead to more drought and heat resilient plants, but also to ecosystems with higher vegetation cover and thus both higher water demands (Donohue et al., 2013, Ukkola et al., 2015) and a greater susceptibility to large fires (Hughes, 2003). Disentangling the potential future influence of these counteracting effects on Australian ecosystems remains a key research priority.

20 **5 Conclusion**

We have shown that extreme events such as the ‘Angry Summer’ 2012 / 2013 can alter the energy balance and therefore mitigate or amplify the event. The woodland sites reduced latent heat flux by stomatal regulation in response to the warm and dry atmospheric conditions. Stronger surface heating in the afternoons then led to an amplification of the surface temperatures. Only the forest site AU-Tum had access to readily available soil water and showed increased latent heat flux. The increased latent heat flux mitigated the effect of the heat wave but continuously depleted the available soil water. The generally increased atmospheric and soil temperatures led to increased respiration and decreased or unchanged net ecosystem productivity. Although all observed ecosystems remained carbon sinks through the duration of the heat wave, the potential exists for positive carbon – climate feedbacks in response to future extreme events, particularly if they increase in duration, intensity or frequency.

30



Appendix A

We have used measurements of a reference period during the same season but one year after the heat wave 2012 / 2013 occurred. Ideally we would have used a climatology derived from observations but OzFlux is a relatively young flux tower network. The first two towers started in 2001 and even globally, very few flux towers have been measuring for more than 15
5 years, which is relatively short compared to typical climatology records of 30-years. To ensure the representativeness of our results we have therefore compared daily data against a climatology derived from BIOS2 output for the time period 1982-2013.

Table A1 shows the agreement between BIOS2 output for all sites and the time period the year 2013. Agreement was generally very good, even more so for the latent heat flux than for the carbon fluxes. Carbon fluxes, and more specifically
10 respiration at the dry Mediterranean woodlands showed stronger disagreement. It is likely that this to some degree reflects night time issues with the eddy covariance method (e.g. van Gorsel, 2009) and with the partitioning of the measured fluxes. This may also be an indication that the model was underestimating drought-tolerance at these sites. The low modeled carbon uptake corresponded to periods of low soil water. There were long periods when the modeled soil water was below wilting
15 point within the entire root zone of 4m. Underestimation could occur if roots were accessing deeper water, the wilting point parameter was too high or the modeled soil water was too low, relative to the wilting point.

Figure A1 shows that during HW1 the latent heat flux at the MW and TW sites was reduced even further. During HW2, precipitation and temporarily increased water availability brought the latent heat flux back to levels observed during BGH. At the temperate forest, however, the latent heat flux strongly increased, particularly during HW1. Increasingly reduced soil water and lower temperatures reduced the effect during HW2.

20 Figure A2 shows that carbon uptake was decreased at MW and TW during HW1 and similar to background conditions during HW2. At TF, the forest site, carbon uptake was increased. Respiration (Fig. A2b) was increased at all locations and during both heat wave periods.

Acknowledgements

This work utilised data from the OzFlux network which is supported by the Australian Terrestrial Ecosystem Research
25 Network (TERN) (<http://www.tern.org.au>) and by grants funded by the Australian Research Council. VRD and EP acknowledge the Education Investment fund and HIE for construction and maintenance of the AU-Cum tower. The Australian Climate Change Science Program supported contributions by EvG and VH, SW was supported by the European Commission's FP7 (Marie Curie International Outgoing Fellowship, grant 300083) and ETH Zurich. VRD acknowledges funding from a Ramón y Cajal fellowship RYC-2012-10970.



References

- Abramowitz, G., Gupta, H., Pitman, A.J., Wang, Y.P., Leuning, R., Cleugh, H. and Hsu, H.-L.: Neural Error Regression Diagnosis (NERD): A tool for model bias identification and prognostic data assimilation, *J Hydrometeorol*, 7, doi: <http://dx.doi.org/10.1175/JHM479.1>, 2006.
- 5
- Beadle, N.C.W.: *The vegetation of Australia*. Cambridge University Press, Cambridge, 1981.
- Barr, A. G., Richardson, A. D., Hollinger, D. Y., Papale, D., Arain, M. A., Black, T. A., Bohrer, G., Dragoni, D., Fischer, M.L., Gu, L., Law, B.E., Margolis, H.A., McCaughey, J.H., Munger, J.W., Oechel, W., Schaeffer, K.: Use of change-point detection for friction-velocity threshold evaluation in eddy-covariance studies, *Agr Forest Meteorol*, 171, doi:10.1016/j.agrformet.2012.11.023, 2013.
- 10
- Beringer, J. and Tapper, N. J.: The influence of subtropical cold fronts on the surface energy balance of a semi-arid site, *J. Arid Environ*, doi:10.1006/jare.1999.0608, 2000.
- 15
- Beringer, J., Hutley, L.B., McHugh, I., Arndt, S.K., Campbell, D., Cleugh, H.A., Cleverly, J., Resco de Dios, V., Eamus, D., Evans, B., Ewenz, C., Grace, P., Griebel, A., Haverd, V., Hinko-Najera, N., Huete, A., Isaac, P., Kannia, K., Leuning, R., Liddell, M.J., Macfarlane, C., Meyer, W., Moore, C., Pendall, E., Phillips, A., Phillips, R.L., Prober, S., Restrepo-Coupe, N., Rutledge, S., Schroeder, I., Silberstein, R., Southall, P., Sun, M., Tapper, N.J., van Gorsel, E., Vote, C., Walker, J. and Wardlaw, T.: An introduction to the Australian and New Zealand flux tower network - OzFlux. *Biogeosciences Discuss.*, submitted, 2016.
- 20
- Black, E., Blackburn, M., Harrison, G., Hoskins, B., Methven, J.: Factors contributing to the summer 2003 European heat wave, *Weather* 59, 217–223, 2004.
- 25
- Bowen, I. S.: The ratio of heat losses by conduction and by evaporation from any water surface., *Phys. Rev.*, 27, 779–787, 1926.
- Bureau of Meteorology: Extreme heat in January 2013. Special Climate Statement 43 , Melbourne. Retrieved from www.bom.gov.au/climate/current/statements/scs43e.pdf, 2013.
- 30
- Chapin, F. S., Woodwell, G. M., Randerson, J. T., Rastetter, E. B., Lovett, G. M., Baldocchi, D. D., Clark, D. a., Harmon, M.E., Schimel, D. S., Valentini, R., Wirth, C., Aber, J. D., Cole, J. J., Goulden, M. L., Harden, J. W., Heimann, M., Howarth,



- R.W., Matson, P. a., McGuire, a. D., Melillo, J. M., Mooney, H. a., Neff, J. C., Houghton, R. a., Pace, M. L., Ryan, M. G., Running, S. W., Sala, O. E., Schlesinger, W. H. and Schulze, E.-D. D.: Reconciling Carbon-cycle Concepts, Terminology, and Methods, *Ecosystems*, 9(7), 1041–1050, doi:10.1007/s10021-005-0105-7, 2006.
- 5 Ciais, P., Reichstein, M., Viovy, N., Granier, A., Ogee, J., Allard, V., Aubinet, M., Buchmann, N., Bernhofer, C., Carrara, A., Chevallier, F., De Noblet, N., Friend, A. D., Friedlingstein, P., Grunwald, T., Heinesch, B., Keronen, P., Knohl, A., Krinner, G., Loustau, D., Manca, G., Matteucci, G., Miglietta, F., Ourcival, J. M., Papale, D., Pilegaard, K., Rambal, S., Seufert, G., Soussana, J. F., Sanz, M. J., Schulze, E. D., Vesala, T., and Valentini, R.: Europe-wide reduction in primary productivity caused by the heat and drought in 2003, *Nature*, 437, 529–533, 2005.
- 10 CSIRO and Bureau of Meteorology: State of the Climate 2014. Retrieved from www.bom.gov.au/state-of-the-climate?documents/state-of-the-climate-2014_low-res.pdf?ref=button, 2014.
- Dai, A.: Increasing drought under global warming in observations and models, *Nature Clim. Change*, 3, 52–58, 2013.
- 15 Dole, R., Hoerling, M., Perlwitz, J., Eischeid, J., Pegion, P., Zhang, T., Quan, X.W., Xu, T. and Murray, D.: Was there a basis for anticipating the 2010 Russian heat wave? *Geophys Res Lett* 38, DOI: 10.1029/2010GL046582, 2011.
- Donohue, R. J., Roderick, M. L., McVicar, T. R. and Farquhar, G. D.: Impact of CO₂ fertilization on maximum foliage cover across the globe's warm, arid environments. *Geophys Res Lett*, 40, 3031–3035, 2013.
- 20 Evans, B., Stone, C. and Barber, B.: Linking a decade of forest declines in southwest, Western Australia to bioclimatic change, *Australian Forestry*, 76, 164–172, 2013.
- 25 Evans, B. and Lyons, T.: Bioclimatic Extremes Drive Forest Mortality in Southwest, Western Australia, *Climate*, 1, 36, 2013.
- Fischer, E. M., Seneviratne, S. I., Vidale, P. L., Lüthi, D., and Schär, C.: Soil Moisture–Atmosphere Interactions during the 2003 European Summer Heat Wave, *J. Clim.*, 20, 5081–5099, 2007.
- 30 Frank, D., Reichstein, M., Bahn, M., Thonicke, K., Frank, D., Mahecha, M.D., Smith, P., Velde, M., Vicca, S., Babst, F., Beer, C., Buchmann, N., Canadell, J.G., Ciais, P., Cramer, W., Ibrom, A., Miglietta, F., Poulter, B., Rammig, A., Seneviratne, S.I. Walz, A., Wattenbach, M., Zawala, M.A., Zscheischler, J.: Effects of climate extremes on the terrestrial



- carbon cycle: concepts, processes and potential future impacts. *Glob Change Biol*, 21, 2861-2880, doi: 10.1111/gcb.12916, 2015.
- Granier, A., Bréda, N., Biron, P. and Villette, S.: A lumped water balance model to evaluate duration and intensity of
5 drought constraints in forest stands. *Ecol Model*, 116, 269-283, 1999.
- Guerlet, S., Basu, S., Butz, A., Krol, M., Hahne, P., Houweling, S., Hasekamp, O.P. and Aben, I.: Reduced carbon uptake during the 2010 Northern Hemisphere summer from GOSAT. *Geophys Res Lett*, DOI: 10.1002/grl.50402, 2013.
- Hanson, C.E., Palutikof, J.P., Dlugolecki, A., Giannakopoulos, C.: Bridging the gap between science and the stakeholder: the
10 case of climate change research. *Climate Res*, 31, doi:10.3354/r031121. 2006.
- Haverd, V. and Cuntz, M.: Soil–Litter–Iso: A one-dimensional model for coupled transport of heat, water and stable isotopes in soil with a litter layer and root extraction, *Journal of Hydrology*, 388, 438-455, 2010.
- 15 Haverd, V., Raupach, M. R., Briggs, P. R., Canadell, J. G., Davis, S. J., Law, R. M., Meyer, C. P., Peters, G. P., Pickett-Heaps, C., and Sherman, B.: The Australian terrestrial carbon budget, *Biogeosciences*, 10, 851-869, 2013a.
- Haverd, V., Raupach, M.R., Briggs, P.R., Canadell, J.G., Isaac, P., Pickett-Heaps, C., Roxburgh, S.H., van Gorsel, E., Viscarra Rossel, R.A. and Wang, Z.: Multiple observation types reduce uncertainty in Australia's terrestrial carbon and water
20 cycles. *Biogeosciences*, 10, 3, 2011-2040, 2013b.
- Hsu, K., Gupta, H.V., Gao, X., Sorooshian S., and Imam, B.: Self-Organizing Linear Output (SOLO): An artificial neural network suitable for hydrological modeling and analysis. *Water Resour Res*, 38, 1302, doi:10.1029/2001WR000795, 2002.
- 25 Hughes, L.: Climate change and Australia: Trends, projections and impacts, *Austral Ecol*, 28, 423–443, 2003.
- IPCC: Climate Change 2013: The Physical Science Basis. Contribution of Working Group I to the Fifth Assessment Report of the Intergovernmental Panel on Climate Change [Stocker, T.F., D. Qin, G.-K. Plattner, M. Tignor, S.K. Allen, J. Boschung, A. Nauels, Y. Xia, V. Bex and P.M. Midgley (eds.)], Cambridge University Press, Cambridge, UK and New
30 York, USA, 2013.
- Isaac P: FluxNet Data OzFlux: Australian and New Zealand Flux Research and Monitoring hdl: 102.100.100/14247, 2015



- Isaac, P., Cleverly, J., Beringer, J., and McHugh, I.: The OzFlux network data path: from collection to curation, *Biogeosciences*, this issue, 2016.
- Keenan, T. F., Hollinger, D.Y., Bohrer, G., Dragoni, D. Munger, J.W., Schmid, H.P. and Richardson A.D.: Increase in
5 forest water-use efficiency as atmospheric carbon dioxide concentrations rise. *Nature* 499, 324–7, 2013.
- King A.D., Karoly D.J., Donat M.G. and Alexander L.V.: Climate change turns Australia’s 2013 Big Dry into a year of record-breaking heat. *B Am Meteorol Soc.*, 95, 41-45, 2014.
- 10 Karoly, D., England, M. and Stiffen W.: Off the charts: Extreme Australian summer heat. Report by the Climate Commission, retrieved from <http://climatecommission.angrygoats.net/report/off-charts-extreme-january-heat-2013/>, 2013.
- Lee, X., Massman, W. and Law, B.E.: *Handbook of micrometeorology. A guide for surface flux measurements and analysis.* Kluwer Academic Press, Dordrecht, 250p., 2004.
- 15 Leuning R., Cleugh H.A., Zegelin S.J. and Hughes D.: Carbon and water fluxes over a temperate Eucalypt forest and a tropical wet/dry savanna in Australia: measurements and comparison with MODIS remote sensing estimates. *Agric For Meteorol*, 129, *Agric For Meteorol*, doi:10.1016/j.agrformet.2004.12.004, 2005.
- 20 Leuning, R., Zegelin, S.J., Jones, K., Keith, H. and Hughes, D.: Measurement of horizontal and vertical advection of CO₂ within a forest canopy, *Agric For Meteorol*, 148, doi:10.1016/j.agrformet.2008.06.006, 2008.
- Lewis, S. C. and King, A. D.: Dramatically increased rate of observed hot record breaking in recent Australian temperatures, *Geophys Res Lett*, 42, 7776-7784, 2015.
- 25 Matusick, G., Ruthrof, K., Brouwers, N., Dell, B. and Hardy, G. J.: Sudden forest canopy collapse corresponding with extreme drought and heat in a mediterranean-type eucalypt forest in southwestern Australia. *Eur J Forest Res*, 132, 497–510, 2013.
- 30 McDowell, N., Pockman, W.T., Allen, C.D., Breshears, D.D., Cobb, N., Kolb, T., Plaut, J., Sperry, J., West, A., Williams, D.G. and Yepez, E.A.: Mechanisms of plant survival and mortality during drought: why do some plants survive while others succumb to drought?. *New phytologist*, doi: 10.1111/j.1469-8137.2008.02436.x., 2008.



- Meyer, W.S., Kondrova, E. and Koerber, G.R.: Evaporation of perennial semi-arid woodland in southeastern Australia is adapted for irregular but common dry periods. *Hydrol Process*, DOI: 10.1002/hyp.10467, 2015.
- Mitchell, P. J., O'Grady, A. P., Hayes, K. R. and Pinkard, E. A.: Exposure of trees to drought-induced die-off is defined by a
5 common climatic threshold across different vegetation types., *Ecol Evol*, 4(7), 1088–101, doi:10.1002/ece3.1008, 2014.
- Oliver, J.E.: Bowen Ratio, *Climatology*, Part of the series *Encyclopedia of Earth Science*, doi: 10.1007/0-387-30749-4_30, 1987.
- 10 Pfautsch, S. and Adams, M. A.: Water flux of Eucalyptus regnans: Defying summer drought and a record heat wave in 2009. *Oecologia*, 172, 317–326. <http://doi.org/10.1007/s00442-012-2494-6>, 2013.
- Reichstein, M., Ciais, P., Papale, D., Valentini, R., Running, S., Viovy, N., Cramer, W., Granier, A., Ogee, J., Allard, V., Aubinet, M., Bernhofer, Chr., Buchmann, N., Carrara, A., Grunwald, T., Heimann, M., Heinesch, B., Knohl, A., Kutsch, W.,
15 Loustau, D., Manca, G., Matteucci, G., Miglietta, G., Ourcival, J.M., Pilegaard, K., Pumpanen, J., Rambal, S., Schapphoff, S., Seufert, G., Soussana, J.F., Sanz, M.J., Vesala, T. and Zhao, M.: Reduction of ecosystem productivity and respiration during the European summer 2003 climate anomaly: a joint flux tower, remote sensing and modelling analysis. *Glob Change Biol*, 13(3), <http://doi.org/10.1111/j.1365-2486.2006.01224.x>, 2007.
- 20 Reichstein, M., Bahn, M., Ciais, P., Frank, D., Mahecha, M. D., Seneviratne, S. I., Zscheischler, J., Beer, C., Buchmann, N., Frank, D. C., Papale, D., Rammig, A., Smith, P., Thonicke, K., van der Velde, M., Vicca, S., Walz, A., and Wattenbach, M.: Climate extremes and the carbon cycle, *Nature*, 500, 287-295, 2013.
- Richardson, A.D., Braswell, B.H., Hollinger, D.Y., Burman, P., Davidson, E.A., Evans, R.S., Flanagan, L.B., Munger, J.W.,
25 Savage, K., Urbanski, S.P. and Wofsy, S.C., 2006. Comparing simple respiration models for eddy flux and dynamic chamber data. *Agr Forest Meteorol*, 141(2), doi:10.1016/j.agrformet.2006.10.010, 2006.
- Schär, C., Vidale, P. L., Luthi, D., Frei, C., Haberli, C., Liniger, M. A., and Appenzeller, C.: The role of increasing temperature variability in European summer heatwaves, *Nature*, 427, 332-336, 2004.
- 30 Schotanus, P., Nieuwstadt F. T. M., and de Bruin H. A. R.: Temperature measurement with a sonic anemometer and its application to heat and moisture fluxes, *Bound Lay Meteor*, 26, 81–93, 1983.



- Seneviratne, S. I., Corti, T., Davin, E. L., Hirschi, M., Jaeger, E. B., Lehner, I., Orlowsky, B., and Teuling, A. J.: Investigating soil moisture-climate interactions in a changing climate: A review, *Earth-Sci. Rev.*, 99, 125-161, 2010.
- Sheffield, J., Wood, E. F., and Roderick, M. L.: Little change in global drought over the past 60 years, *Nature*, 491, 435-438,
5 2012.
- Steffen, W.: Quantifying the impact of climate change on extreme heat in Australia. Report by the Climate Council of Australia, retrieved from <http://www.climatecouncil.org.au/uploads/00ca18a19ff194252940f7e3c58da254.pdf>, 2015.
- 10 Steffen, W., Hughes, L. and Perkins, S.: Heatwaves: hotter, longer, more often. Report by the Climate Council of Australia, retrieved from <http://www.climatecouncil.org.au/uploads/9901f6614a2cac7b2b888f55b4dff9cc.pdf>, 2014.
- Sun, Q., Meyer, W.S., Koerber, G.R. and Marschner, P.: Response of respiration and nutrient availability to drying and rewetting in soil from a semi-arid woodland depends on vegetation patch and a recent wildfire, *Biogeosciences*, DOI: 10.5194/bg-12-5093-2015, 2015.
15
- Tanner, C. B. and Thurtell, G. W.: Anemoclinometer measurements of Reynolds stress and heat transport in the atmospheric surface layer, Research and Development Tech. Report ECOM 66-G22-F to the US Army Electronics Command, Dept. Soil Science, Univ. of Wisconsin, Madison, WI, 1969.
20
- Teuling, A.J., Seneviratne, S.I., Stöckli, R., Reichstein, M., Moors, E., Ciais, P., Luysaert, S., van den Hurk, B., Ammann, C., Bernhofer, C. and Dellwik, E., Gianelle, D., Gielen, B., Grünwald, Th., Klumpp, K., Montagnani, L., Moureaux, Ch., Sottocornola, M. and Wohlfahrt, G.: Contrasting response of European forest and grassland energy exchange to heatwaves. *Nature Geoscience*, 3, doi: 10.1038/NGEO950, 2010.
25
- Tuzet, A., Perrier, A. and Leuning, R.: A coupled model of stomatal conductance, photosynthesis and transpiration. *Plant, Cell and Environment*, 1097–1116, 2003.
- Ukkola, A. M. Prentice, I.C., Keenan, T.F., van Dijk, A.I., Viney, N.R., Myneni, R.B. and Bi, J.: Reduced streamflow in
30 water-stressed climates consistent with CO₂ effects on vegetation. *Nat Clim Chang* 6, 75–78, 2015.
- van Gorsel, E., Leuning, R., Cleugh, H.A., Keith, H. and Suni, T., 2007: Nocturnal carbon efflux: Reconciliation of eddy covariance and chamber measurements using an alternative to the u^* -threshold filtering technique, *Tellus B*, 59, doi: 10.1111/j.1600-0889.2007.00252.x, 2007.
35



- van Gorsel, E., Delpierre, N., Leuning, R., Black, A., Munger, J.W., Wofsy, S., Aubinet, M., Feigenwinter, Ch., Beringer, J., Bonal, D., Chen, B., Chen, J., Clement, R., Davis, K.J., Desai, A.R., Dragoni, D., Etzold, S., Grünwald, T., Gu, L., Heinesch, B., Hutrya, L.R., Jans, W.W.P., Kutsch, W., Law, B.E., Leclerc, M.Y., Mammarella, I., Montagnani, L., Noormets, A., Rebmann, C. and Wharton S.: Estimating nocturnal ecosystem respiration from the vertical turbulent flux and change in storage of CO₂, *Agric For Meteorol*, 149, doi:10.1016/j.agrformet.2009.06.020, 2009.
- 5
- van Gorsel, E., Berni, J.A.J., Briggs, P., Cabello-Leblic, A., Chasmer, L., Cleugh, H.A., Hacker, J., Hantson, S., Haverd, V., Hughes, D. and Hopkinson, C., Keith, H., Kljun, N., Leuning, R., Yebra, M. and Zegelin, S.: Primary and secondary effects of climate variability on net ecosystem carbon exchange in an evergreen Eucalyptus forest, *Agric For Meteorol*, 182, doi:10.1016/j.agrformet.2013.04.027, 2013.
- 10
- Wang, Y. P., Law, R. M., and Pak, B.: A global model of carbon, nitrogen and phosphorus cycles for the terrestrial biosphere, *Biogeosciences*, 7, 2261-2282, 2010.
- 15
- Wang, Y.P., Kowalczyk, E., Leuning, R., Abramowitz, G., Raupach, M.R., Pak, B., van Gorsel, E., Luhar, A.: Diagnosing errors in a land surface model (CABLE) in the time and frequency domains, *J Geophys Res*, 116, doi: 10.1029/2010JG001385, 2011.
- 20
- Webb, E., Pearman, G. and Leuning R.: Correction of flux measurements for density effects due to heat and water vapor transfer, *Q J Roy Meteor Soc*, 106, 85–100, 1980.
- 25
- Wesely, M., 1970: Eddy correlation measurements in the atmospheric surface layer over agricultural crops. Ph. D. Dissertation, 102pp., 1970.
- 30
- Whan, K., Zscheischler, J., Orth, R., Shongwe, M., Rahimi, M., Asare, E.O. and Seneviratne, S.I.: Impact of soil moisture on extreme maximum temperatures in Europe. *Weather and Climate Extremes*, 9, 57-67, 2015
- Wolf, S., Eugster, W., Ammann, C., Häni, M., Zielis, S., Hiller, R., Stieger, J., Imer, D., Merbold, L., and Buchmann, N.: Contrasting response of grassland versus forest carbon and water fluxes to spring drought in Switzerland, *Environ. Res. Lett.*, 8, 035007, 2013.
- 30
- Wolf S, Keenan TF, Fisher JB, Baldocchi DD, Desai AR, Richardson AD, Scott RL, Law BE, Litvak ME, Brunsell NA, Peters W, van der Laan-Luijkx IT: Warm spring reduced carbon cycle impact of the 2012 US summer drought, 2016. DOI



10.1073/pnas.1519620113

Wolf S, Yin D, Roderick ML: Using radiative signature to diagnose the cause of warming associated with the Californian Drought. *Journal of Geophysical Research - Atmospheres*, in review

5

Yuan, W., Cai, W., Chen, Y., Liu, S., Dong, W., Zhang, H., Yu, G., Chen, Z., He, H., Guo, W., Liu, D., Liu, S., Xiang, W., Xie, Z., Zhao, Z. and Zhou, G.: Severe summer heatwave and drought strongly reduced carbon uptake in Southern China. *Scientific Reports - Nature*, 18813. <http://doi.org/10.1038/srep18813>, 2015.

- 10 Zhao, M. and Running, S. W.: Drought-Induced Reduction in Global Terrestrial Net Primary Production from 2000 Through 2009. *Science*, 329(5994), 940–943. <http://doi.org/10.1126/science.1192666>, 2010.

Zimmermann, N. E., N. G. Yoccoz, T. C. Edwards, E. S. Meier, W. Thuiller, A. Guisan, et al. 2009. Climatic extremes improve predictions of spatial patterns of tree species. *Proc Natl Acad Sci*, 106, 19723–19728, 2009.

15

Zhu, Z., Bi, J., Pan, Y., Ganguly, S., Anav, A., Xu, L., Samanta, A., Piao, S., Nemani, R.R., Myneni, R.B.: Global Data Sets of Vegetation Leaf Area Index (LAI)_{3g} and Fraction of Photosynthetically Active Radiation (FPAR)_{3g} Derived from Global Inventory Modeling and Mapping Studies (GIMMS) Normalized Difference Vegetation Index (NDVI_{3g}) for the Period 1981 to 2011, *Remote Sens.*, 5, doi:10.3390/rs5020927, 2013.

20

Zscheischler, J., Orth, R. and Seneviratne, S.I.: A submonthly database for detecting changes in vegetation - atmosphere coupling. *Geophys Res Lett*, DOI: 10.1002/2015gl066563, 2015.



Figures



Figure 1. Map indicating the locations of the OzFlux sites used in this study. The sites are grouped into three distinct climate and ecosystem types, indicated by red dots for Mediterranean woodlands (MW), light green dots for temperate woodlands (TW) and dark green dots for temperate forest (TF)

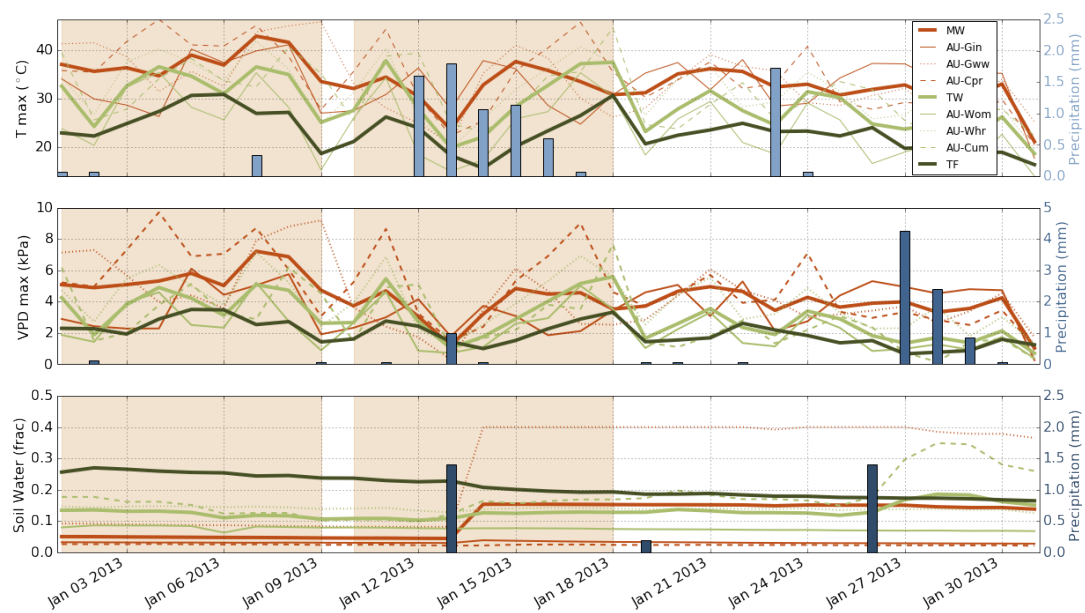
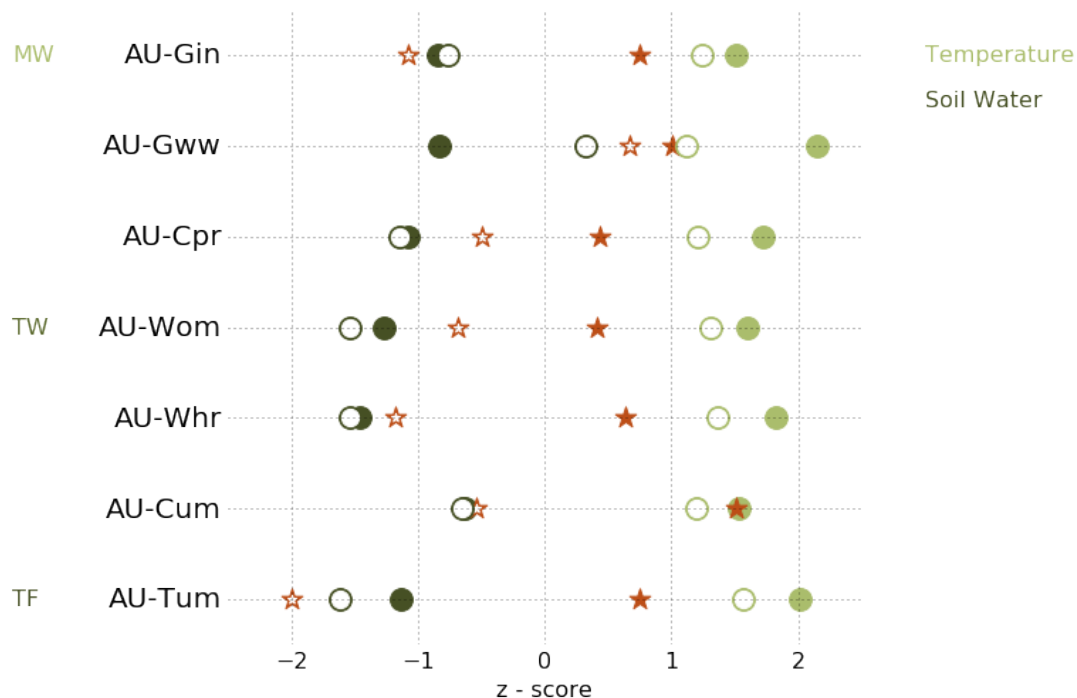


Figure 2. Time series of daily maximum temperature (T, top panel), vapour pressure deficit (VPD, middle panel) and soil water (lowest panel). The legend is given in top panel. Precipitation (P) is given as the average of the daily cumulated precipitation of the sites and displayed for each biome in one panel: Light blue colours indicate the Mediterranean



woodlands (MW, AU-Gin, AU-Gww and AU-Cpr, panel 1), middle blue the temperate woodlands (TW, AU-Wom, AU-Whroo and AU-Cum, panel 2) and dark blue the temperate forest (TF, AU-Tum, panel 3).



5 Figure 3. z-scores for temperature and soil water across flux tower sites. Solid red stars denote temperature and non filled red stars denote soil water scores during the background period (BGH) compared to the climatological background BGC. Scores for temperature and soil water for HW1 and HW2 compared to the same time periods in the years 1982-2013 are shown for HW1 (1/1/2013–9/1/2013) by filled dots and for HW2 (10/1/2013–18/1/2013) by non-filled dots.

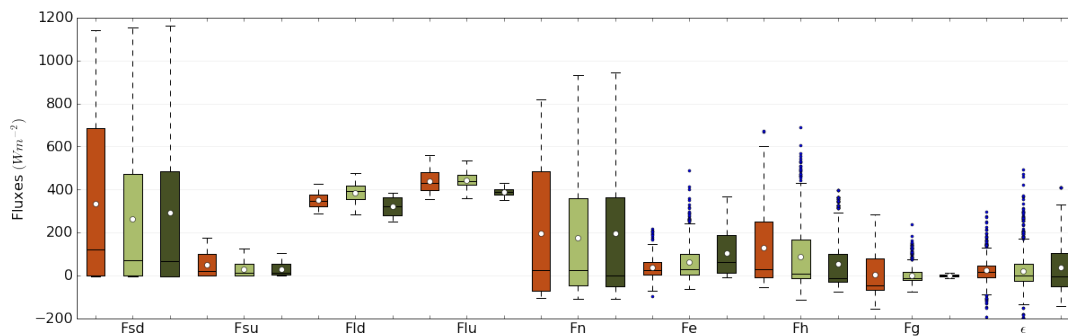


Figure 4. Box plot of energy fluxes for Mediterranean woodlands (MW, red), temperate woodlands (TW, light green) and temperate forests (TF, dark green). Energy fluxes are incoming shortwave radiation (Fsd), reflected shortwave radiation (Fsu), downward longwave radiation (Fld), emitted longwave radiation (Flu), net radiation (Fn), latent heat flux (Fe), sensible heat flux (Fh), ground heat flux (Fg) and energy imbalance (ϵ) during the background period BGH (2/1/2014 – 6/1/2014). The box extends from the lower to upper quartile values of the data, with a line at the median. The mean value is indicated with a dot. The whiskers extend from the box to show the range of the data. Flier points are those past the end of the whiskers.

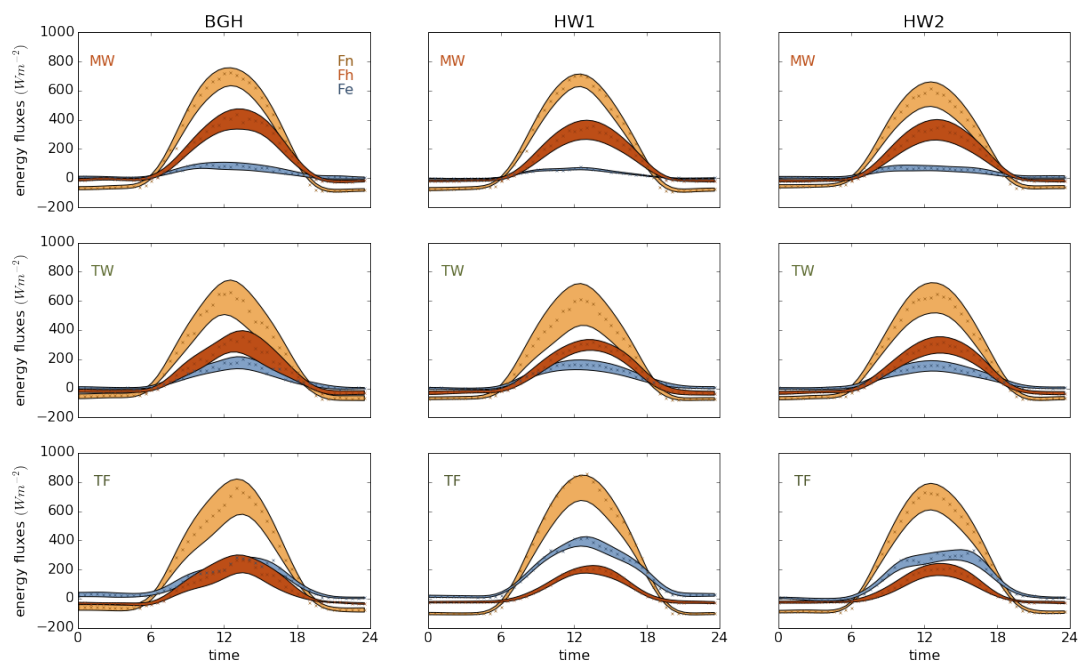


Figure 5. Diurnal course of net radiation (Fn, light amber), sensible (Fh, dark amber) and latent (Fe, blue) heat at the Mediterranean woodlands (MW, top row), the temperate woodlands (TW, middle row) and the temperate forest (TF, lowest row) for the background period BGH (2/1/2014 – 6/1/2014), and the first and second period of the heat wave (HW1 (1/1/2013–9/1/2013), HW2 (10/1/2013–18/1/2013)). Filled areas indicate the range of smoothed ± 1 standard deviation, average mean values are indicated by symbols.

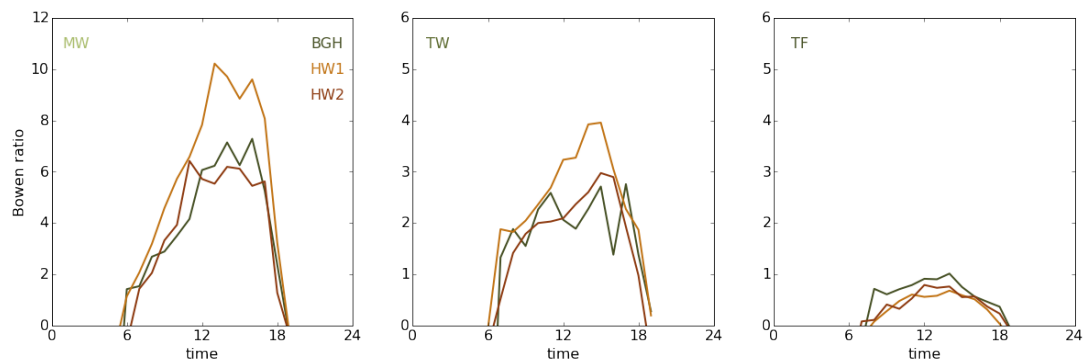


Figure 6. Daytime Bowen ratio measured over Mediterranean woodlands (MW, left panel), the temperate woodlands (TW, middle panel) and the temperate forest (TF, right panel) for BGH (green line), HW1 (light amber) and HW2 (dark amber).

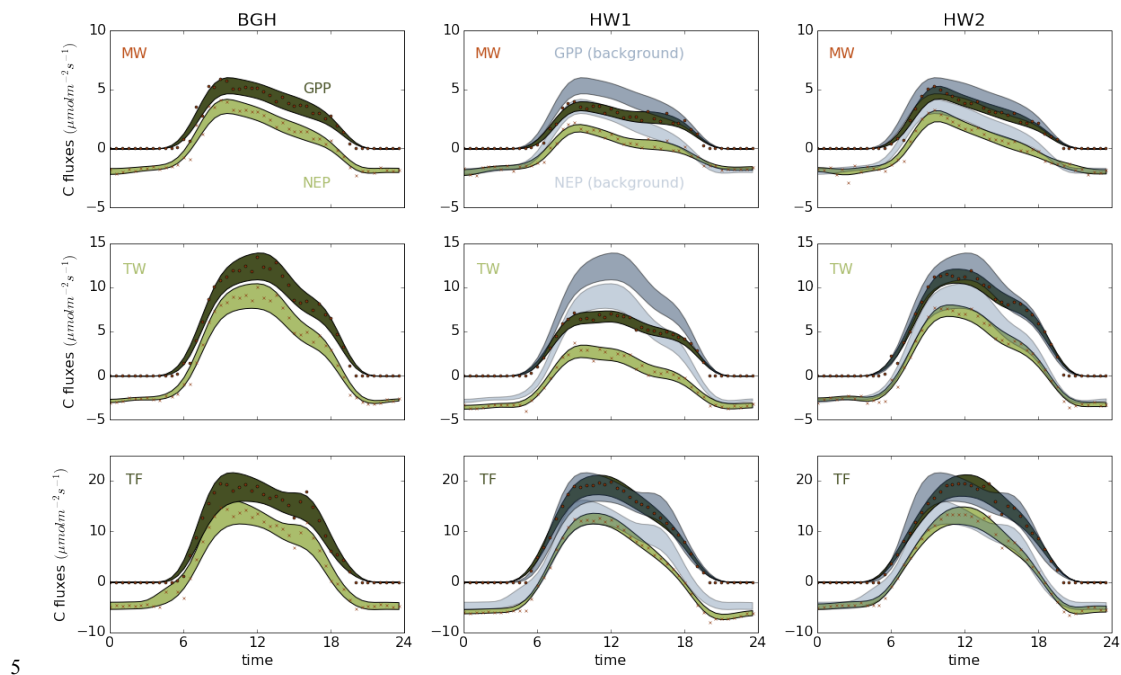


Figure 7. Diurnal course of net ecosystem productivity (NEP, light green) and gross primary productivity (GPP, dark green) heat at the Mediterranean woodlands (MW, top row), the temperate woodlands (TW, middle row) and the temperate forest



(TF, lowest row) for the background period (BGH), and the first and second period of the heat wave (HW1, HW2). Filled areas indicate the range of smoothed ± 1 standard deviation values, average mean values are indicated by red symbols. Background GPP values (dark grey) and NEP values (light grey) are also plotted in HW1 and HW2 to allow for easier comparison.

5

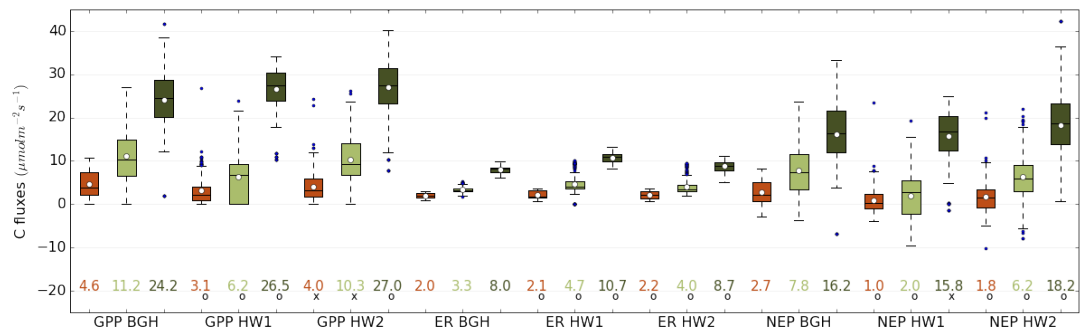


Figure 8. Boxplot of daytime values (9:00-16:00 local standard time) of gross primary productivity (GPP), ecosystem respiration (ER) and net ecosystem productivity (NEP) for the background period (BGH) and the first and second period of the heat wave (HW1, HW2). Mean values are given below boxes and symbols indicate that they are significantly different

10 from the background period (o) or not (x).

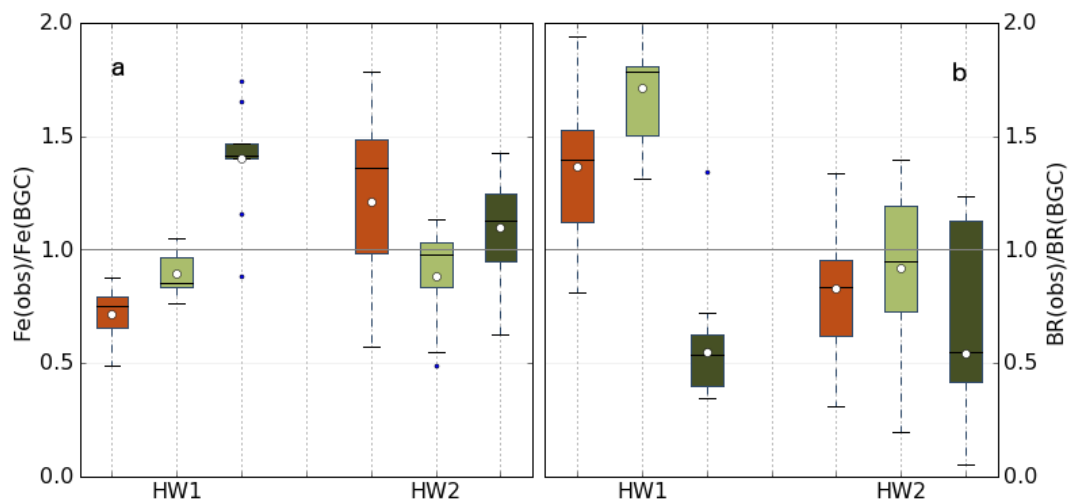


Figure A1. Left panel: Boxplot of the ratio of observed latent heat ($Fe(obs)$) to the climatology of the latent heat flux ($Fe(BGC)$) during the first and second period of the heat wave (HW1, HW2). Right panel: same as left but for the Bowen ratio.

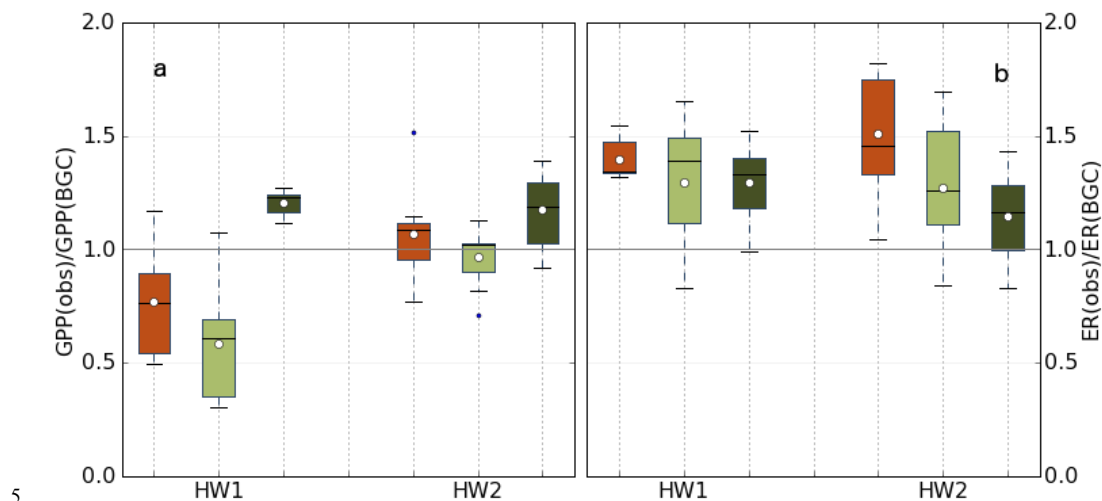


Figure A2. Left panel: Boxplot of the ratio of observed gross primary productivity ($GPP(obs)$) to the climatology of GPP ($GPP(BGC)$) during the first and second period of the heat wave (HW1, HW2). Right panel: same as left but for the ER.



Tables

Table 1. List of OzFlux sites used in this study, abbreviations and site information. MW stands for Mediterranean woodlands, TW for temperate woodlands and TF for temperate forest. MAT and MAP are the mean annual temperature and precipitation for the years 1982-2013 (BIOS2).

ID	Site Name	Latitude (deg)	Longitude (deg)	Elevation (m)	MAT (C)	MAP (mm)	LAI Modis (m ² /m ²)	Tree Height (m)	Biome
AU-Gin	Gingin	-31.375	115.714	51	18.4	681	0.9	7	MW
AU-Gww	Great Western Woodlands	-30.192	120.654	450	18.7	396	0.4	25	MW
AU-Cpr	Calperum	-34.004	140.588	67	17.0	265	0.5	4	MW
AU-Wom	Wombat	-37.422	144.094	702	11.4	936	4.1	25	TW
AU-Whr	Whroo	-36.673	145.029	155	14.6	533	0.9	30	TW
AU-Cum	Cumberland Planes	-33.613	150.723	33	17.6	818	1.3	23	TW
AU-Tum	Tumbarumba	-35.657	148.152	1260	9.8	1417	4.1	40	TF



Table 2. Climatology of radiation and energy exchange for the ecosystems Mediterranean Woodlands (MW), Temperate Woodlands (TW) and Temperate Forests (TF) and the variables flux of shortwave downward radiation (F_{sd}), shortwave upward radiation (F_{su}), longwave downward radiation (F_{ld}), longwave upward radiation (F_{lu}), net radiation (F_n), latent heat (F_c), sensible heat (F_h), ground heat (F_g) and the energy imbalance (ϵ). Where values during the two periods of the heat wave ($\Delta HW1$ and $\Delta HW2$) differ significantly from the background (BGH) ($P < 0.1$) this is indicated by bold fonts.

	MW	TW	TF	MW	TW	TF	MW	TW	TF	MW	TW	TF	MW	TW	TF	MW	TW	TF	MW	TW	TF	MW	TW	TF			
	F_{sd}			F_{su}			F_{ld}			F_{lu}			F_n			F_c			F_h			F_g			ϵ		
BGH	335	264	293	49	30	31	350	383	323	439	444	387	197	175	197	38	63	103	130	90	55	5	1	0	24	21	39
ΔHW_1	-10	4	70	-1	0	3	38	9	0	49	33	41	-19	-20	26	-12	2	52	-5	30	-8	6	4	5	-8	-56	-23
ΔHW_2	-62	20	16	-10	2	14	36	2	-13	19	16	12	-35	3	-8	-3	-2	14	-29	-4	-8	-5	1	0	1	8	-14



Table A1. Parameters of robust linear model fit between observations and BIOS2 output for all sites, the variables latent heat flux (F_e), gross primary productivity (GPP), ecosystem respiration (ER) and the time interval 1/1/2013 – 31/12/2013.

variable	ID	coeff	stderr	[95% conf. int.]		RMSE	r^2
F_e	AU-Gin	0.9998	5.87e-06	1.000	1.000	27.52	0.44
	AU-Gww	0.9285	0.0032	0.867	0.990	23.13	0.58
	AU-Cpr	0.7464	0.032	0.684	0.809	15.75	0.41
	AU-Wom	1.1253	0.017	1.093	1.158	18.55	0.89
	AU-Whr	0.8917	0.031	0.830	0.953	23.66	0.42
	AU-Cum	1.0385	0.020	0.999	1.078	28.75	0.53
	AU-Tum	0.8121	0.014	0.784	0.840	36.61	0.65
GPP	AU-Gin	1.0570	0.035	0.988	1.126	1.91	0.42
	AU-Gww	0.3496	0.031	0.290	0.410	0.95	0.15
	AU-Cpr	0.2806	0.021	0.240	0.321	1.06	0.10
	AU-Wom	1.0176	0.015	0.988	1.047	1.53	0.81
	AU-Whr	1.0194	0.037	0.947	1.092	2.32	0.38
	AU-Cum	1.8764	0.037	1.803	1.949	2.81	0.48
	AU-Tum	0.6667	0.006	0.655	0.679	3.20	0.88
ER	AU-Gin	1.1687	0.043	1.084	1.253	2.20	0.13



AU-Gww	0.4483	0.015	0.420	0.477	0.66	0.31
AU-Cpr	0.3492	0.013	0.324	0.374	0.73	0.01
AU-Wom	1.2682	0.035	1.199	1.337	2.56	0.48
AU-Whr	1.4227	0.039	1.347	1.499	1.87	0.14
AU-Cum	2.0017	0.031	1.941	2.063	2.62	0.66
AU-Tum	0.8770	0.013	0.852	0.902	1.69	0.77